

# Investigating the effect of MgO and CeO<sub>2</sub> on the crystallization behavior of ZrO<sub>2</sub> in Li<sub>2</sub>O- SiO<sub>2</sub>- ZrO<sub>2</sub> glass in order to prepare a dental base

**Z.S. Ghoreishy Madise<sup>1</sup>, B. Eftekhari Yekta<sup>1\*</sup>**

( \* [BEftekhari@iust.ac.ir](mailto:BEftekhari@iust.ac.ir) )

## Abstract

ZrO<sub>2</sub> is commonly incorporated into ceramic glass substrates to enhance radiopacity, mechanical strength, and chemical durability. Experience has shown that the crystallization of tetragonal zirconia in glass will have a greater effect on the mechanical properties of ceramic glass. To achieve optimal properties in zirconia, stabilizing oxides are often added to enhance its structural and mechanical qualities. In this research, in order to stabilize the tetragonal phase of zirconia, MgO and CeO<sub>2</sub> were added to the glass ceramic composition of the Li<sub>2</sub>O-SiO<sub>2</sub>-ZrO<sub>2</sub> system and the desired dental substrate was synthesized through the sinter process. The behavior of sintering and crystallization of basic and optimized glass was investigated using HSM and DTA thermal analysis, respectively. The results showed that the optimal sinter temperature, heat press and heat treatment are equal to 730°C, 900°C and 825°C, respectively. Then, in order to determine the crystallization behavior of the prepared samples, X-ray diffraction and microstructure images were used. The results also showed that the presence of the main Li<sub>2</sub>ZrSi<sub>6</sub>O<sub>15</sub> phase crystallizes at a temperature of 825°C in the base sample and the sample containing ceria. Also, due to early formation of MgSiO<sub>3</sub> crystals, magnesia prevents sintering and formation of Li<sub>2</sub>ZrSi<sub>6</sub>O<sub>15</sub> phase and stability of tetragonal zirconia phase. In the sample containing ceria, during crystallization, ZrO<sub>2</sub> entered its crystal structure and led to the stability of the tetragonal zirconia phase at room temperature.

**Keywords :** Glass ceramic, Dental glass ceramic, stabilized zirconia, IPS Empress Cosmo.

---

1 School of Metallurgy and Materials Engineering, Iran University of Science and Technology, Tehran, Iran.

## Introduction

When the tooth needs nerve extraction, there is a possibility that the crown of the tooth will be lost. In such conditions, according to (Fig.1-a), the presence of a core is necessary to create a base for the veneer, and the dental core itself needs a post inside the canal is the root [1]. Nowadays, because of their beauty and non-sensitivity, ceramics have replaced metal-based dental restorations [2]. After developing the  $ZrO_2$  post, a blank was required to be placed on the  $ZrO_2$ . To fulfill this need,  $Li_2O-SiO_2-ZrO_2$  glass ceramics with the IPS Empress Cosmo brand were developed by Schweiger et al [3]. This ceramic glass is placed on the  $ZrO_2$  post through a heat press, on which a lucite ceramic glass crown may be placed Taked [4-5]. Therefore, according to (Fig.1-b), the whole dental blind post system consists of a single product consisting of a stabilized  $ZrO_2$  ceramic (CosmoPost), and a glass ceramic containing  $ZrO_2$  (IPS Empress Cosmo). As a result, there are two completely different substances that are combined and form a product in a specific process. The composition and microstructure of ceramic glass containing  $ZrO_2$  after heat pressing at  $900\text{ }^\circ\text{C}$  is characterized by crystals rich in  $ZrO_2$ . These crystals are  $Li_2ZrSi_6O_{15}$  [6-9]. Zirconia-based ceramics have attracted special attention in the last two decades due to their unique properties (high toughness, high mechanical strength, corrosion resistance, fracture resistance, etc.). Pure zirconia is a polymorphic substance; This means that during heating and cooling, its crystal lattice changes. Based on this, monoclinic zirconia is stable from zero to  $1170\text{ }^\circ\text{C}$ , tetragonal zirconia is stable from  $1170\text{ }^\circ\text{C}$  to  $2170\text{ }^\circ\text{C}$ , and cubic zirconia is stable from  $2170\text{ }^\circ\text{C}$  to the melting point ( $2680\text{ }^\circ\text{C}$ ). Tetragonal to monoclinic transformation occurs at a temperature of about  $1170\text{ }^\circ\text{C}$ , which is accompanied by a volume expansion of about 3-5% [9]. Also, during heating, the monoclinic phase transforms into tetragonal, and this is accompanied by a decrease in volume of about 9-10% [10]. The stresses caused by these expansions and contractions cause cracks to appear in pure zirconia, which causes the ceramics made of this material to crumble during cooling from the sinter temperature or heating to This temperature becomes Stabilized zirconia by using some metal oxides such as  $CaO$ ,  $MgO$ ,  $In_2O_3$ ,  $Sc_2O_3$ ,  $CeO_2$  and  $Y_2O_3$  prevents phase transformation and stabilizes the tetragonal zirconia phase at room temperature and eliminates volume changes [11-12]. In this research, the effect of the presence of stabilizers in IPS Empress Cosmo glass ceramic composition and microstructure investigation has been discussed.

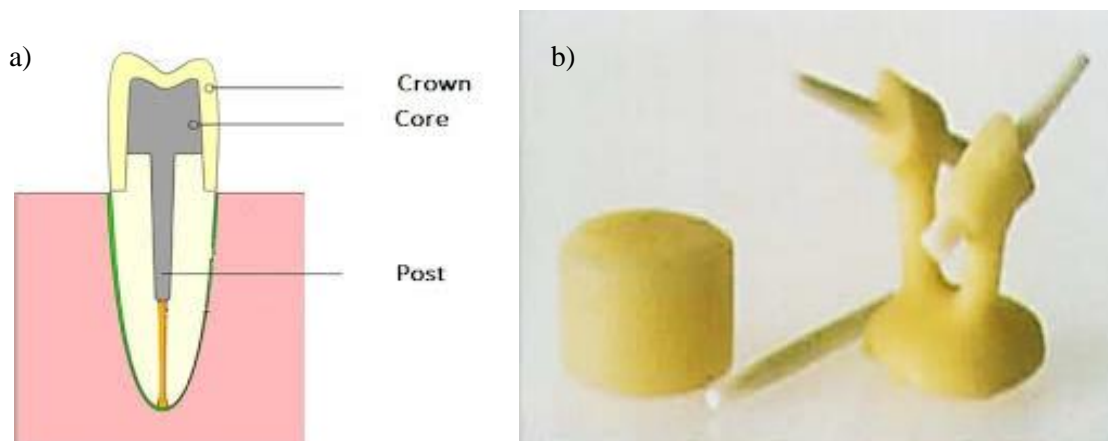


Fig.1-a. Schematic of a post core and cover b) CosmoPost cylindrical post with conical tip and IPS Empress Cosmo core, produced using the heat press method.

### Research materials and methods

Three glass compositions  $G_0$ ,  $G_1$  and  $G_2$  were prepared according to Table 1.  $G_0$  glass was used as a basic composition without any stabilizer, and  $G_1$  and  $G_2$  compositions included ceria and magnesia, respectively, to investigate the role of stabilizer in it.

Table 1. Weight composition of the three studied glasses

	SiO <sub>2</sub>	Li <sub>2</sub> O	ZrO <sub>2</sub>	P <sub>2</sub> O <sub>5</sub>	Al <sub>2</sub> O <sub>3</sub>	Na <sub>2</sub> O	K <sub>2</sub> O	F	CeO <sub>2</sub>	MgO
$G_0$	58.7	8	15.2	4.2	5	3.2	4.8	1	-	-
$G_1$	58.7	8	15.2	4.2	5	3.2	4.8	1	11.8	-
$G_2$	58.7	8	15.2	4.2	5	3.2	4.8	1	-	11.8

Material the first consumption, Silica (Merck No.1.13126) Lithium carbonate (Merck No.1.05671), zirconia (Merck No.1.00757), phosphorus pentoxide (Merck No.1.00540), aluminum oxide (Merck No.1.01095), Carbonate sodium (Merck No.1.06392), nitrate potassium (Merck No.1.05061), cryolite (Merck No.1.06457), cerium oxide (Merck No.1.02263), Magnesium oxide (Merck No.1.05865), was Ferrite was prepared from compounds  $G_0$ ,  $G_1$  and  $G_2$  in a silicon crucible at a temperature of 1450 °C in an AZAR-F3L0271 furnace. Then it was ground by a Chinese mortar to the average particle size equal to  $d_{50} = 10\mu\text{m}$ , and in order to investigate the sintering behavior of the glass, the dimensional in the Thermal were first measured changes of the pressed powder Microscope (HSM)<sup>1</sup> Model Solution System Expert - ODHT HSM Misura It was investigated with a heating rate 10°C/min up to a temperature of 1000°C Observed and recorded. The crystallization behavior of the powders was investigated by differential thermal analysis (DTA) with a Polymer Laboratories-

<sup>1</sup> Hot stage microscope

1640 device and with the same heating pattern as a thermal microscope. From the ground powders, tablets with a diameter of 17 mm were prepared under a press pressure of 50 MPa. The X-ray Diffraction (XRD) test was done by Bruker Germany D8 advance machine between 5-90 angles and scanning electron microscope (SEM) test by Tescan Czech Republic - mira3 device done.

## Results and discussion

It is shown in (Fig.2) the DTA diagram, the absence of sharp peaks in this diagram indicates the surface crystallization of this compound.

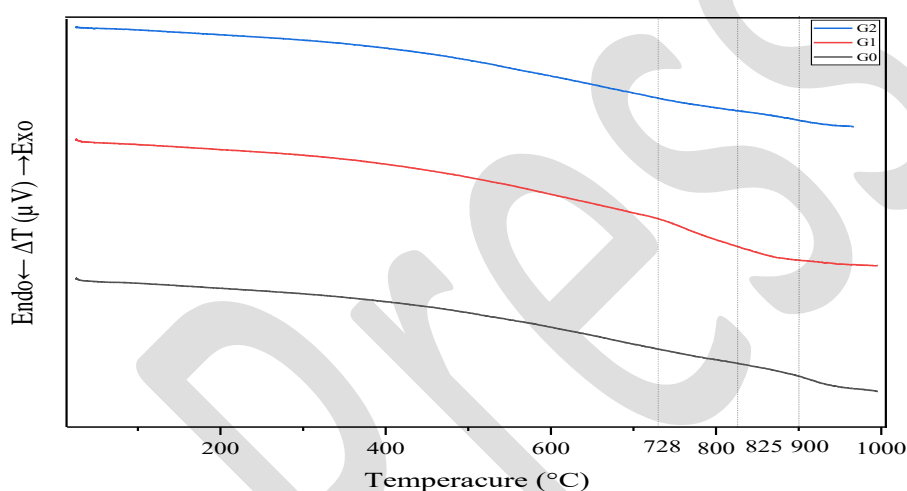


Fig. 2. Images of thermal analysis of DTA curve of three compound G<sub>0</sub>, G<sub>1</sub> and G<sub>2</sub>.

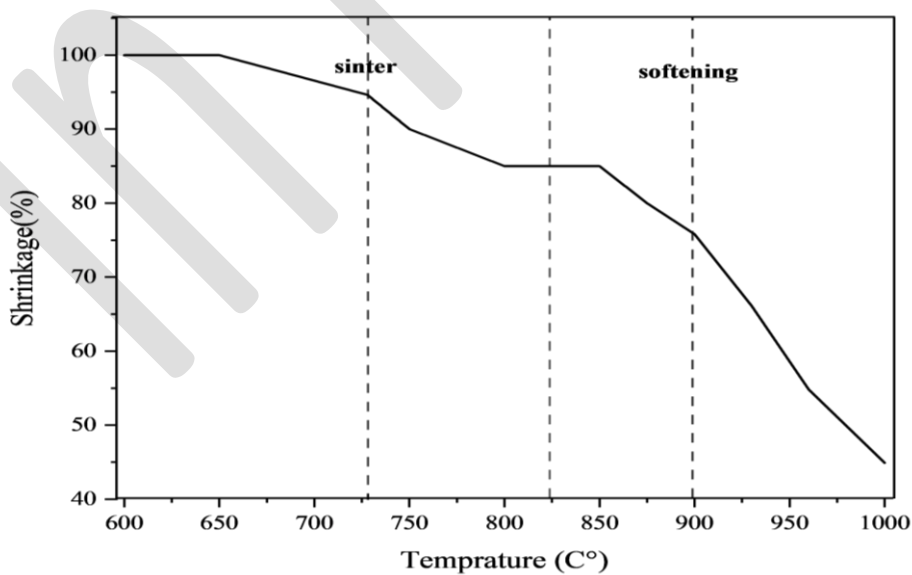
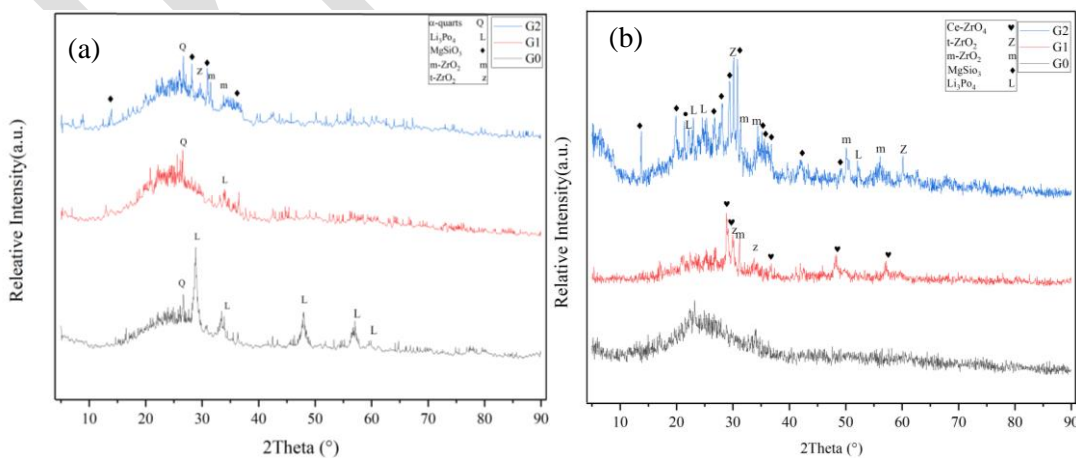


Fig.3. HSM curve G<sub>0</sub> composition

In order to accurately check the sinter temperature, HSM analysis was used. Instantaneous dimensional changes of glasses with increasing temperature were observed in a thermal microscope, and based on that, the length change curves according to temperature were drawn in (Fig.3). According to this curve, the maximum shrinkage of the sample starts at a temperature of about 700°C. Then, the shrinkage of the sample increases with a steep slope, until the shrinkage stops at a temperature close to 800-850°C. After that, contraction continues again. The total shrinkage from the ambient temperature to 1000°C is equal to 60%, according to (Fig.3), the sintering temperature was shown to be 728°C. The tablets were heat treated at this temperature for 2 hours and its XRD pattern was (Fig.4-a) is shown. Also, the percentage of shrinkage is constant in the temperature range of 800-850°C, the stopping of shrinkage from the temperature of 800-850°C for this glass can be attributed to the beginning of crystallization in them, for this reason, the samples at the temperature They were heat treated at 825°C with a heating rate of 10°C/min for 2 hours. The XRD pattern of this sample can be seen in (Figure 4-c). Also, according to the dental application of ceramic glass, the base of this ceramic glass is subjected to heat press forming operation to form the main phase ( $\text{Li}_2\text{O}\cdot\text{ZrO}_2\cdot 6\text{SiO}_2$ )  $\text{Li}_2\text{ZrSi}_6\text{O}_{15}$  under heat pressing operation [8]. According to the effect of low pressure in the formation of this phase and according to (Fig.3) which shows the softening temperature of this ceramic glass equal to 900°C, the sintered tablets at the temperature of 728°C at the softening temperature with the heating rate 10°C/min was placed in the heat treatment furnace for 20 minutes. The XRD pattern is shown in (Fig.4-b).



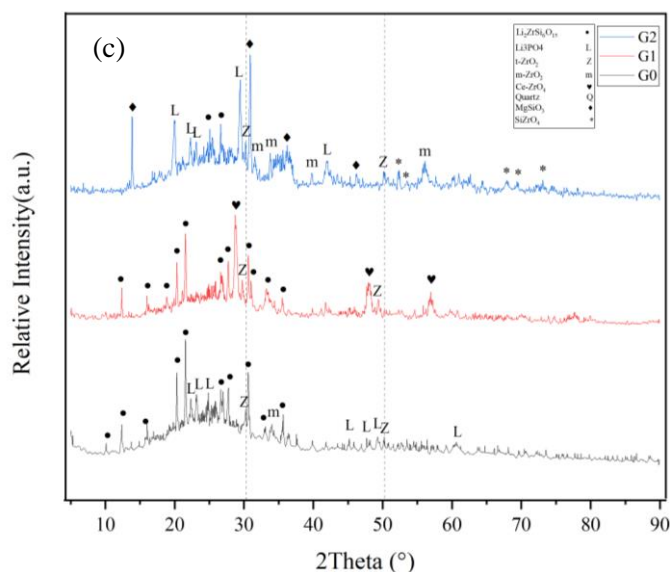


Fig.4. XRD images of three compounds  $G_0$ ,  $G_1$  and  $G_2$  a) sintered at  $728^\circ\text{C}$  for 2 hours. b) Sintered at  $728^\circ\text{C}$  for 2 hours and heat treated at  $900^\circ\text{C}$  for 20 minutes. c) Heat treatment at  $825^\circ\text{C}$  for 2 hours

After heat treatment at  $728^\circ\text{C}$  (Fig.4-a), the sample containing ceria is sintered well and has a high linear contraction, for this reason many crystalline phases cannot be seen in its XRD pattern. In the base sample, the main crystalline phase consisted of very small  $\text{Li}_3\text{PO}_4$  crystals, these crystals were formed in a droplet phase that was rich in phosphate by separating the liquid-liquid phase in the glass, as a result, these droplets grew by heat treatment did or were placed together and finally formed very small crystals of  $\text{Li}_3\text{PO}_4$ , it can be seen that this phase also plays a nucleating role for the phase containing  $\text{ZrO}_2$ . In the sample containing magnesia, the  $\text{MgSiO}_3$  phase crystallizes faster than other phases and causes the lack of sinterability of this sample, also monoclinic and tetragonal zirconia are seen, which is caused by the lack of stability of the zirconia phase in this composition. The quartz peak at this temperature is caused by crushing in the porcelain mortar. In (Fig.4-b) and (Fig.5-a) the  $G_0$  sample is seen as amorphous and there is no crystalline phase, according to (Fig.1) and the presence of the Endo peak around  $900^\circ\text{C}$ , phase dissolution has occurred. The accurate matching of the temperature can be attributed to the error of the STA device or the temperature gradient of the furnace at this temperature the sample was deformed. In sample  $G_1$ , the main phase is  $\text{Ce-ZrO}_4$  (Fig.5-b) and after that, tetragonal zirconia phase can be seen at  $2\Theta=29/85^\circ$  and  $2\Theta=34^\circ$ , since no peak is seen in the base sample. the peak shift is not comparable to check the stability. This sample was also deformed like the base sample. The sample  $G_2$  was not deformed, also lamination had occurred in this sample. In this sample, like the tablets that were placed at the annealing temperature, the main phase was  $\text{MgSiO}_3$ , and

$\text{Li}_3\text{PO}_4$  crystals can also be seen, which were eaten by acid in (Fig.5-c). has beenThe next phase is monoclinic zirconia, which is caused by the lack of effect of magnesia as a stabilizer in this composition. In general, despite the expectation [3], the simulated heat press operation in the base sample caused phase dissolution and also prevented the formation of  $\text{Li}_2\text{ZrSi}_6\text{O}_{15}$  phase in all samples.

By examining the diagram of the thermal microscope and the contraction stopping in the temperature range of 800-850°C, there is a possibility of crystallization starting at this temperature. For this purpose, in order to check the crystallized phase, it was heat treated at an intermediate temperature of 825°C for two hours, according to (Fig.4-c) and (Fig.5-d) in sample  $G_0$ ,  $\text{Li}_2\text{ZrSi}_6\text{O}_{15}$  phase is formed, also tetragonal zirconia is seen at angles of  $2\Theta=30/22^\circ$  and  $2\Theta=50/24^\circ$  respectively with intensity of 90 and 50. Also, monoclinic zirconia along with lithium phosphate can be seen in this sample. The mentioned data are consistent with the results of Schweinger et al. [3], despite the fact that in the above experiment, after heat pressing at 900°C, the mentioned phases were obtained. The presence of this phase at this temperature and without heat pressing makes the production process of Cosmo ceramic glass one-step. In sample  $G_1$ , the  $\text{Li}_3\text{PO}_4$  phase is not seen, this sample is deformed and melted after being placed at this temperature, in the melting state, the crystalline phase dissolves in the glass, and the  $\text{Li}_3\text{PO}_4$  phase is completely dissolved in this sample. (Fig.5-e). Due to the faster formation of Ce-ZrO<sub>4</sub> compared to ZrO<sub>2</sub>, ZrO<sub>2</sub> peaks were consumed and tetragonal zirconia peaks were formed with less intensity compared to the base sample. It is seen with intensity of 70 and 45 respectively. After comparing this sample with the  $G_0$  sample, we see the shift of the peak to the left, which is caused by the presence of ceria in the zirconia structure. Due to having a smaller ionic radius (0.82 Å) of  $\text{Zr}^{4+}$  compared to (0.97 Å) of  $\text{Ce}^{4+}$ , according to the relationship  $n\lambda=2d\sin\Theta$ , as  $d$  increases,  $\sin\Theta$  decreases and  $\Theta$  also decreases, causing the peak to shift to the left. Also, the absence of monoclinic zirconia phase is due to stabilization of tetragonal zirconia phase in this sample. Sample  $G_2$  includes peaks of monoclinic zirconia, tetragonal zirconia and  $\text{MgSiO}_3$ . The presence of monoclinic zirconia in this composition is due to the instability of the tetragonal phase, but to further investigate the shift of the tetragonal zirconia peak, we also examined it. The ionic radius of  $\text{Mg}^{4+}$ , like the atomic radius of  $\text{Zr}^{4+}$ , is equal to 0.72 Å and the peak shift should be to the right. At the angles of  $2\Theta=30/22^\circ$  and  $2\Theta=50/24^\circ$  with an intensity of 90, 50 tetragonal zirconia is seen, which corresponds to the base sample. Also, in this sample, contrary to other temperatures and other samples, zircon phase (Fig.5-j) is seen.

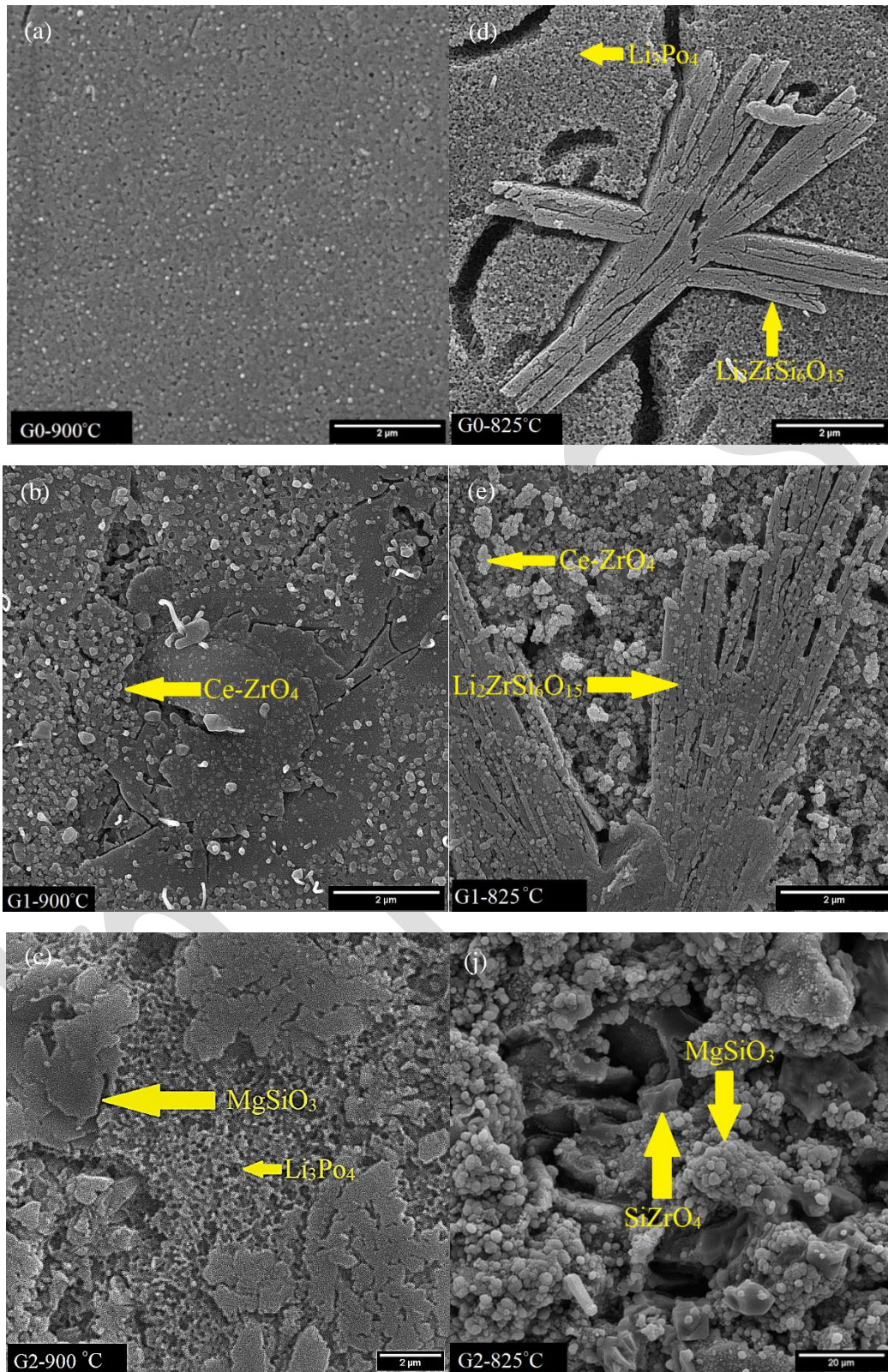


Fig.5. SEM images of samples chemically etched with 3% HF for 12 seconds and heat treated at 900°C for 20 minutes, a) G<sub>0</sub>, b) G<sub>1</sub>, c) G<sub>2</sub> and heat treated at 825°C for 20 minutes 2 hours, d) G<sub>0</sub>, e) G<sub>1</sub>, j) G<sub>2</sub>.



According to (Fig.5-a), with re-heat treatment of the base sample at softening temperature or heat press at 900 °C, despite the report of Holland et al.[8] It is with DTA and XRD data. In the sample containing ceria (Fig5-b) with heat treatment at 900 °C, small Ce-ZrO<sub>4</sub> crystals were seen. The zirconia phase could not be seen due to its fineness. In the sample containing magnesia (Fig.5-c), MgSiO<sub>3</sub> crystals were seen. In this sample, the crystalline phase of Li<sub>3</sub>PO<sub>4</sub> was corroded by chemical etching, and cavities with spherical morphology due to the loss of Li<sub>3</sub>PO<sub>4</sub> crystals were seen. Despite the previous studies of heat press operation, Li<sub>2</sub>ZrSi<sub>6</sub>O<sub>15</sub> phase was not created in any of the samples. SEM images of samples heat treated at 825°C showed the presence of Li<sub>2</sub>ZrSi<sub>6</sub>O<sub>15</sub> phase with snowflake-like morphology in base samples and samples containing ceria (Fig.5-d and 5-e). The presence of this phase in the sample containing ceria is larger than the base sample. Also, in the basic sample (Fig.5-c), the Li<sub>3</sub>PO<sub>4</sub> phase has been destroyed due to chemical etching and caused the presence of holes. In the sample containing ceria, in addition to the Li<sub>2</sub>ZrSi<sub>6</sub>O<sub>15</sub> phase, Ce-ZrO<sub>4</sub> crystals were also seen (Fig.5-e). In G<sub>2</sub>-825°C sample, unlike the other two samples, it was not sintered and did not have linear contraction, for this reason, large MgSiO<sub>3</sub> and SiZrO<sub>4</sub> crystals were visible in this sample (Fig.5-j). Also, monoclinic and tetragonal ZrO<sub>2</sub> crystals were not seen by SEM in all samples due to their small size.

## conclusion

According to the XRD and SEM test results, re-heat treatment causes phase dissolution in the base sample and lack of formation of Li<sub>2</sub>ZrSi<sub>6</sub>O<sub>15</sub> main phase. According to the HSM chart, the shrinkage at 825°C is due to the formation of Li<sub>2</sub>ZrSi<sub>6</sub>O<sub>15</sub> phase, for this reason, this temperature is the optimal heat treatment temperature. The presence of ceria in the sample heat treated at 825°C caused the stability of the tetragonal zirconia phase in this sample because no peak containing monoclinic zirconia was seen in this sample, and also in the XRD pattern, the shift of the tetragonal zirconia peak to the left compared to the base sample and also We can see the decrease in the intensity of the peak, which is caused by the presence of ceria in the structure of zirconia, in the base sample and the sample containing magnesia, we see the presence of monoclinic zirconia, which indicates the lack of stability of the zirconia phase in these two samples, as well as early crystallization. MgSiO<sub>3</sub> prevents sintering of this sample.

## References

- [1] R. Madan, S. Phogat, K. Bhatia, P. Malhotra, G. Bhatia, "A step ahead in post and core technique for patients with limited interarch space," *Saint's Int. Dent. J.*, 2016, 2(1), 17-20.
- [2] H.R Rezaie, H. Beigi Rizi, M. Mahdi Rezaie Khamseh, A. Öchsner, *Dental Restorative Materials*, chapter3, A review on dental materials, Springer Cham, Switzerland, 2020, 47-171.
- [3] M. Schweiger, M. Frank, S. Cramer Von Clausbruch, V. Rheinberger, "Microstructure and properties of a composite system for dental applications composed of glass-ceramics in the  $\text{SiO}_2$ - $\text{Li}_2\text{O}$ - $\text{ZrO}_2$ - $\text{P}_2\text{O}_5$  system and  $\text{ZrO}_2$ -ceramic (TZP)," *Journal of materials science*, 1999, 34, 4563 – 4572.
- [4] M. Montazerian, E. Dutra Zanotto, "History and trends of bioactive glass-ceramics," *Biomed. Mater. Res. Part A*, 2016, 104(5), 1231–1249.
- [5] W. Höland, V. Rheinberger, E. Apel, C. van 't Hoen, M. Höland, A. Dommann, M. Obrecht, C. Mauth, U. Graf-Hausner, "Clinical applications of glass-ceramics in dentistry," *Mater. Sci. Mater. Med*, 2006, 17(11), 1037–1042.
- [6] S. Saadaldin, A. Rizkalla, "Glass-Ceramics for Non-Metallic Dental Implant Applications," 2013 .
- [7] M. Montazerian, ED Zanotto, *Restorative Dental Glass-Ceramics: Current Status and Trends*, chapter 9, Clinical Applications of Biomaterials, Springer Cham, Switzerland, 2017, 313–336.
- [8] W. Holland, G Beall, *Composition Systems for Glass-Ceramics*, chapter 2, *Glass-Ceramic Technology*, John Wiley & Sons, Inc., Hoboken, New Jersey, 2019, 170-172.
- [9] J.A Brito-Chaparro, A. Aguilar-Elguezabal, J. Echeberria, MH Bocanegra-Bernal, "Using high-purity MgO nanopowder as a stabilizer in two different particle size monoclinic  $\text{ZrO}_2$  : Its influence on the fracture toughness, *Materials Chemistry and Physics*, 2009, 114(1), 407–414.
- [10] Shrikant V. Joshi, M.P. Srivastava, "On the thermal cycling life of plasma-sprayed yttria-stabilized zirconia coatings," *Surf. Coatings Technol*, 1993, 56(3), 215–224.
- [11] R. Shoja Razavi, M.R. Loghman-Estarki, *Techniques for the Synthesis of Nanostructured Zirconia-Based Ceramics for Thermal Barrier Application*, chapter1, sol-gel Based Nanoceramic Materials: Preparation, Properties and Applications, Springer Cham, Switzerland, 2017, 21–91.
- [12] Wijayanti, R. Berliana, I. Rosmayanti, K. Wahyudi, E. Maryani, H. Hernawan, R. Septawendar, "Preparation of magnesia partially stabilized zirconia nanomaterials from zirconium hydroxide and magnesium carbonate precursors using peg as a template," *Crystals*, 2021, 11, 635.